

## Configuration-interaction description of transition-metal impurities in II-VI semiconductors

T. Mizokawa and A. Fujimori

*Department of Physics, University of Tokyo, Bunkyo-ku, Tokyo 113, Japan*

(Received 23 July 1993)

The electronic properties of substitutional  $3d$  transition-metal impurities in II-VI semiconductors have been studied using the cluster and Anderson impurity models with configuration interaction. It is shown that the photoemission and inverse-photoemission spectra,  $d$ - $d$  optical-absorption spectra, exchange interaction between the  $3d$  magnetic moment and the host band states, and donor and acceptor ionization energies can be reproduced with the same set of parameters, which show systematic variation with expected chemical trends. The importance of multiplet effects in the formation of donor and acceptor levels within the band gap is demonstrated.

### I. INTRODUCTION

$3d$  transition-metal impurities in semiconductors have attracted much interest from their technological importance as well as from the viewpoint of basic physics. Apparently paradoxical experimental results have been obtained from different experimental techniques.<sup>1</sup> Optical-absorption spectra<sup>1-10</sup> have a series of weak, sharp features due to intra-atomic  $d$ - $d$  transition and have been analyzed by ligand-field theory,<sup>11,12</sup> indicating that the  $3d$  electrons are essentially localized. Donor and acceptor ionization energies deduced from transport measurements and charge-transfer optical absorption show variation suggestive of multiplet effects.<sup>1,2</sup> On the other hand, the reduction of hyperfine-coupling constants relative to free ions in electron-spin double-resonance spectra and superhyperfine interaction in electron-nuclear-spin double-resonance spectra suggest that the  $3d$  electrons are delocalized through strong hybridization with the host band states, and have been successfully reproduced by first-principles calculations using the local-density approximation (LDA).<sup>1,13,14</sup> Haldane and Anderson<sup>15</sup> have shown using the unrestricted Hartree-Fock (HF) approximation that under the strong hybridization multiple charges states are formed within the band gap of the host semiconductor. There have been some attempts to describe the ionization energies and  $d$ - $d$  transitions energies starting from the HF or LDA solutions.<sup>1,13,14,16</sup> For example, LDA calculations corrected for self-interaction have been extensively made by Zunger to calculate the donor and acceptor ionization energies.<sup>1</sup> Recently, photoemission studies on diluted magnetic semiconductors<sup>17</sup> such as  $\text{Cd}_{1-x}\text{Mn}_x\text{Te}$  have shown that the hybridization is quite substantial as predicted by the LDA calculations whereas there are also multielectron satellite features which cannot be explained by one-electron theories.<sup>18,19</sup> In order to explain the photoemission spectra, cluster<sup>19</sup> and Anderson impurity models<sup>20</sup> with configuration interaction (CI) have been introduced. The latter models start from the ionic configuration and include ligand-to- $3d$  charge-transferred configurations in a CI formalism. In the light of the various physical pictures emerging from the different experiments and different theories, it is

highly desirable to construct a coherent picture in which one can explain the various experimental data in a unified way.

In this paper, we have applied CI theory to the analysis of a variety of experimental data and shown that the CI picture can indeed give a unified description of the electronic properties of the  $3d$  transition-metal impurities. The organization of this paper is as follows. A brief description of the CI picture is given in Sec. II. In Secs. III A–III C, we present the results of  $d$ - $d$  absorption spectra, photoemission and inverse-photoemission spectra, and exchange constants between the  $3d$  magnetic moment and the host band states obtained from the cluster model calculations. In Sec. IV D, donor and acceptor ionization energies are calculated using the Anderson impurity model.

### II. CONFIGURATION-INTERACTION APPROACH

In the CI picture, the wave functions of the ground state and charge-conserving excited states, which we call  $N$ -electron states, are spanned by the  $d^n, d^{n+1}\underline{L}, \dots, d^{10}\underline{L}^{10-n}$  configurations, where  $\underline{L}$  denotes a hole in the valence band for the Anderson impurity model or a hole in a ligand  $p$  orbital for the cluster model. The ligand-to- $3d$  charge-transfer energy is defined by  $\Delta \equiv E(d^{n+1}\underline{L}) - E(d^n)$  and the  $3d$ - $3d$  Coulomb interaction energy by  $U \equiv E(d^{n-1} + E(d^{n+1}) - 2E(d^n))$ , where  $E(d^{n'}\underline{L}^{m'})$  is the center of gravity of the  $d^{n'}\underline{L}^{m'}$  multiplet. This definition, from which the multiplet effect is excluded, makes clear the systematic variation of the parameters on cation atomic number and formal valence.<sup>21</sup> Alternatively, the charge-transfer and Coulomb interaction energies can be defined with respect to the lowest term of each multiplet, and are denoted by  $\Delta_{\text{eff}}$  and  $U_{\text{eff}}$ , respectively. Note that the actual energy required for the acceptor ionization process  $d^n \rightarrow d^{n+1} + \underline{L}$  is determined by  $\Delta_{\text{eff}}$  rather than  $\Delta$ . The multiplet splittings are given in terms of Racah  $B$ ,  $C$  parameters, which are fixed to the free-ion values.<sup>12</sup>

The energy of the ground state  $E_0(N)$  of the neutral impurity ( $A^0$ ) as well as those of the excited  $d^n$  multiplet terms are obtained by diagonalizing the Hamiltonian in

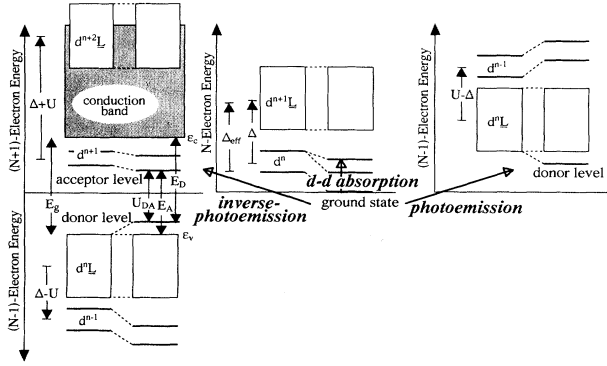


FIG. 1. Schematic energy-level diagrams from a  $d$  transition-metal impurity in a II-VI semiconductor, including hybridization between the  $3d$  and host valence band. For clarity, higher-order charge-transfer states (e.g.,  $d^{n+2}\underline{L}^2$  in the  $N$ -electron states) are not shown.

the  $N$ -electron subspace as shown in the central panel of Fig. 1. In the right panel of Fig. 1, we show the energy levels of the  $(N-1)$  electron states (positively ionized impurity,  $A^+$ ), namely, the final states of photoemission which are given by linear combinations of  $d^{n-1}$ ,  $d^n\underline{L}$ ,  $d^{n+1}\underline{L}^2$ , etc. The lowest-energy level of the  $(N-1)$  electron system is the first ionization level of the  $N$ -electron system or the donor level; the donor ionization energy is given by  $E_0(N-1) - E_0(N) + \varepsilon_c$  ( $\equiv E_D$ ), where  $\varepsilon_c$  is the energy of the conduction-band minimum. The energy levels for the  $(N+1)$ -electron states (negatively ionized impurity,  $A^-$ ) are shown in the left panel of Fig. 1. The lowest-energy level of the  $(N+1)$ -electron system is the affinity level of the  $N$ -electron system or the acceptor level; the acceptor ionization energy is given by  $E_0(N+1) - E_0(N) - \varepsilon_v$  ( $\equiv E_A$ ), where  $\varepsilon_v$  is the energy of the valence-band maximum. If we replot the electron removal energies  $E(N-1) - E_0(N)$  downward and combine it with the electron addition energies  $E(N+1) - E_0(N)$  as in the left panel of Fig. 1, we can effectively map the many-electron energies onto the one-electron energy-level scheme.

### III. RESULTS

#### A. $d-d$ optical-absorption spectra

In order to analyze the valence-band photoemission and  $d-d$  optical-absorption spectra of  $M^{2+}$  ( $A^0$ ) impurities substituting cation sites in II-VI semiconductors, we have performed CI calculations on a tetrahedral  $(MX_4)^{6-}$  cluster model ( $X=S, \text{Se}, \text{or Te}$ ).<sup>19,22,23</sup> One-electron transfer integrals between the  $3d$  orbitals and the ligand orbitals are expressed in terms of Slater-Koster parameters  $(pd\sigma)$  and  $(pd\pi)$ :<sup>24</sup>  $T_{t_2} \equiv \langle t_2 | h | L_{t_2} \rangle = \sqrt{4/3}(pd\sigma)^2 + 8/9(pd\pi)^2$  and  $T_e \equiv \langle e | h | L_e \rangle = 2\sqrt{6}/3(pd\pi)$ , where  $L_{t_2}$  and  $L_e$  are ligand orbitals with  $T_2$  and  $E$  symmetry of the  $T_d$  point group, respectively. In order to reproduce the  $d-d$  optical-absorption spectra

using the same  $\Delta$  and  $U$  as those for the valence-band photoemission spectra, the transfer integrals had to be taken larger than those for the photoemission spectra,<sup>22</sup> indicating that the transfer integrals for the  $N$ -electron system are larger than those for the  $(N-1)$ -electron system. Indeed, Gunnarsson and Jepsen have shown that the transfer integrals depend on the local electronic configuration significantly.<sup>25</sup> Following their results, we have assumed that the transfer integrals between  $d^{n-1}$  and  $d^n\underline{L}$  are smaller by  $\sim 20\%$  and those between  $d^{n+1}$  and  $d^{n+2}\underline{L}$  larger by  $\sim 20\%$  than those between  $d^n$  and  $d^{n+1}\underline{L}$ . Parameter values for  $d^n - d^{n+1}\underline{L}$  are given in this paper.

In Fig. 2, the  $d-d$  optical-absorption spectra of  $\text{MnO}$ ,<sup>26</sup> where the  $\text{Mn}^{2+}$  ion is octahedrally coordinated by six  $\text{O}^{2-}$  ions, and  $\text{Mn}^{2+}$  ( $d^5: A^0$ ) impurities in  $\text{ZnS}$ ,<sup>3</sup>  $\text{ZnSe}$ ,<sup>4</sup> and  $\text{CdTe}$  (Ref. 5) are compared with the result of CI cluster-model calculations. Here, we compare the calculated multiplet structures with the energies of absorption maxima in the spectra which correspond to the purely electronic (Frank-Condon) transition energies. The ground state of the  $\text{Mn}^{2+}$  impurity is  ${}^6A_1$  in the tetrahedral as well as in the octahedral coordination geometry. The energy levels for the lowest excited terms  ${}^4T_1$ ,  ${}^4T_2$ ,  ${}^4A_1$ , and  ${}^4E$ , which originate from the  ${}^4G$  term of the free  $d^5$  ion, are in good agreement with experiment. Agreement is less satisfactory for the higher-energy terms  ${}^4E$ ,  ${}^4T_1$ , and  ${}^4T_2$ , which are derived from the  ${}^4D$  and  ${}^4P$  terms, because the energy levels of the  ${}^4D$  and  ${}^4P$  of the free  $d^5$  ion already cannot be accurately reproduced within the Racah parameter scheme. The obtained parameter sets are listed in Table I, where one can see that in going from S to Se to Te the charge-transfer energy  $\Delta$  decreases as the electronegativity of the ligand decreases and that the transfer integral  $(pd\sigma)$  also decreases as the distance between the transition-metal cation and the ligand anions increases.<sup>24</sup> The effects of the decrease in  $\Delta$  and in  $(pd\sigma)$  cancel to yield the almost identical  ${}^6A_1 - {}^4T_1$  separation for the  $\text{ZnS}$ ,  $\text{ZnSe}$ , and  $\text{CdTe}$  hosts, consistent with the experimental results. We have also performed CI cluster-model calculations for various transition-metal impurities, V to Ni, in  $\text{ZnS}$  and  $\text{ZnSe}$ . The  $d-d$  optical-absorption spectra<sup>3,6-10</sup> are compared with the CI cluster-model calculations in Fig. 3 for the  $\text{ZnS}$  host. The obtained parameters are listed in Table II. The calculated  $d-d$  transition energies are generally in good agreement with the experimental results. Agreement for the  ${}^4T_1$  level of  $\text{Co}^{2+}$  and the  ${}^3T_1$  level of  $\text{Cr}^{2+}$  is less satisfactory because the energy level of  ${}^4P$  for the free  $d^7$  ion and that of  ${}^3P$  for the free  $d^4$  ion already

TABLE I. Parameters used to calculate the valence-band photoemission and inverse photoemission spectra and  $d-d$  optical-absorption spectra (in eV).

|   | $\Delta$ | $U$ | $(pd\sigma)$ |
|---|----------|-----|--------------|
| MnO   | 7.0      | 5.5 | 1.5          |
| $\text{Cd}_{1-x}\text{Mn}_x\text{S}/\text{Cd}_{1-x}\text{Mn}_x\text{S}$   | 3.0      | 4.0 | 1.3          |
| $\text{Cd}_{1-x}\text{Mn}_x\text{Se}/\text{Cd}_{1-x}\text{Mn}_x\text{Se}$ | 2.5      | 4.0 | 1.2          |
| $\text{Cd}_{1-x}\text{Mn}_x\text{Te}$                                     | 2.0      | 4.0 | 1.1          |

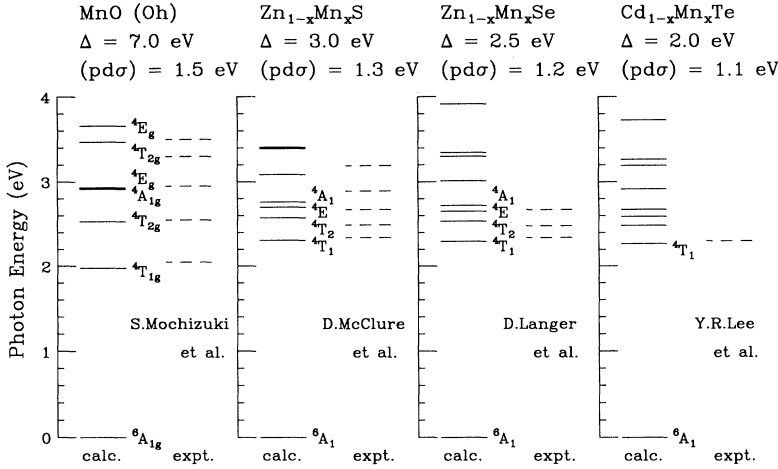


FIG. 2. Energy levels for  $\text{Mn}^{2+}$  ( $A^0$ ) impurities in II-VI semiconductors and MnO calculated using the CI cluster model compared with experimental  $d-d$  optical-absorption spectra (Refs. 3–5 and 26).

cannot be reproduced well within the Racah parameter scheme. The  $\Delta$  values thus obtained monotonically decrease in going from lighter to heavier transition-metal atoms as expected from chemical trends whereas  $\Delta_{\text{eff}}$  exhibits nonmonotonic behavior due to the multiplet effects.<sup>21,27</sup>

### B. Photoemission and inverse-photoemission spectra

In Fig. 4, we compare the Mn  $3d$ -derived photoemission spectra of  $\text{Cd}_{1-x}\text{Mn}_x\text{Y}$  ( $Y = \text{S}, \text{Se}, \text{Te}$ ) (Refs. 18 and 19) with those calculated using the CI cluster model. In contrast to the  $d-d$  optical-absorption spectra, the changes in  $\Delta$  and  $(pd\sigma)$  with ligand atoms affect the photoemission spectra constructively because the energy-level ordering of the ionic ( $d^5$  and  $d^4$ ) and charge-transfer ( $d^6\bar{L}$  or  $d^5\bar{L}$ ) configurations is inverted in going from the  $N$ -electron to the  $(N-1)$ -electron states: In going from S to Se to Te, the intensity within  $\sim 2.5$  eV of the valence-band maximum relative to the main peak at  $\sim 3.4$  eV decreases and that of the satellite at 5–9 eV increases. These observations are well reproduced with the same parameter sets obtained from the  $d-d$  optical-absorption spectra given in Table I.

As for the inverse-photoemission spectra, the Mn  $3d$ -derived structure  $\sim 4.8$  eV above the valence-band maximum<sup>28</sup> is also reproduced by the CI cluster-model calculation as shown in Fig. 5 whereas in band-structure calculations<sup>29</sup> it is predicted to be  $\sim 2$  eV above the valence-

band maximum. The failure of the band-structure calculation is due to the neglect of the Coulomb contribution to the Mn  $3d\uparrow-3d\downarrow$  splitting, resulting in the too small  $d-d$  splitting.

### C. Exchange constants

The exchange constant  $N\beta$  between the  $\text{Mn}^{2+}$  magnetic moment and the Bloch electron at the valence-band maximum of  $\text{Cd}_{1-x}\text{Mn}_x\text{Y}$  ( $Y = \text{S}, \text{Se}, \text{Te}$ ) is derived from magneto-optical effects.<sup>17</sup> In the second-order perturbation with respect to the charge transfer, the  $N\beta$  is given by

$$N\beta \simeq -(16/S)[1/(U_{\text{eff}} - \Delta_{\text{eff}}) + 1/\Delta_{\text{eff}}] \times [1/3(pd\sigma) - 2/9\sqrt{3}(pd\pi)]^2 \quad (1)$$

( $S = 5/2$ ).<sup>30</sup> The  $N\beta$  values for S, Se, and Te evaluated using the above parameters are  $-1.40$ ,  $-1.14$ , and  $-0.95$ , which are in good agreement with the experimental results,  $-1.8$ ,  $-1.11$ , and  $-0.88$  for  $Y = \text{S}, \text{Se},$  and  $\text{Te}$ , respectively.<sup>17</sup> Here, the values for the  $N$ -electron state are used for  $(pd\sigma)$  and  $(pd\pi)$  since  $N\beta$  is obtained from optical measurements where the number of electrons in the system is conserved. In Ref. 30,  $\epsilon_v - \epsilon_d \sim 3.4$  eV instead of  $\Delta_{\text{eff}}$  has been used in Eq. (1) for Mn compounds, where  $\epsilon_d$  is the position of the main peak in the

TABLE II. Parameters used to calculate the  $d-d$  optical-absorption spectra of neutral ( $\text{Mn}^{2+}; A^0$ ) transition-metal impurities in ZnS and ZnSe (in eV). Racah  $B$  and  $C$  parameters are fixed to the values of free ions (Ref. 12).

|                  | $B$   | $C$   | ZnS                                |              | ZnSe                               |              |
|------------------|-------|-------|------------------------------------|--------------|------------------------------------|--------------|
|                  |       |       | $\Delta$ ( $\Delta_{\text{eff}}$ ) | $(pd\sigma)$ | $\Delta$ ( $\Delta_{\text{eff}}$ ) | $(pd\sigma)$ |
| $\text{Ni}^{2+}$ | 0.135 | 0.600 | 1.0 (2.3)                          | 1.2          | 0.5 (1.8)                          | 1.1          |
| $\text{Co}^{2+}$ | 0.138 | 0.541 | 1.5 (2.9)                          | 1.1          | 1.0 (2.4)                          | 1.0          |
| $\text{Fe}^{2+}$ | 0.131 | 0.484 | 2.0 (3.3)                          | 1.2          | 1.5 (2.8)                          | 1.05         |
| $\text{Mn}^{2+}$ | 0.119 | 0.412 | 3.0 (5.2)                          | 1.3          | 2.5 (4.7)                          | 1.2          |
| $\text{Cr}^{2+}$ | 0.103 | 0.425 | 4.0 (1.9)                          | 1.2          | 3.5 (1.4)                          | 1.1          |
| $\text{V}^{2+}$  | 0.095 | 0.354 | 4.5 (3.6)                          | 1.3          | 4.0 (3.1)                          | 1.2          |

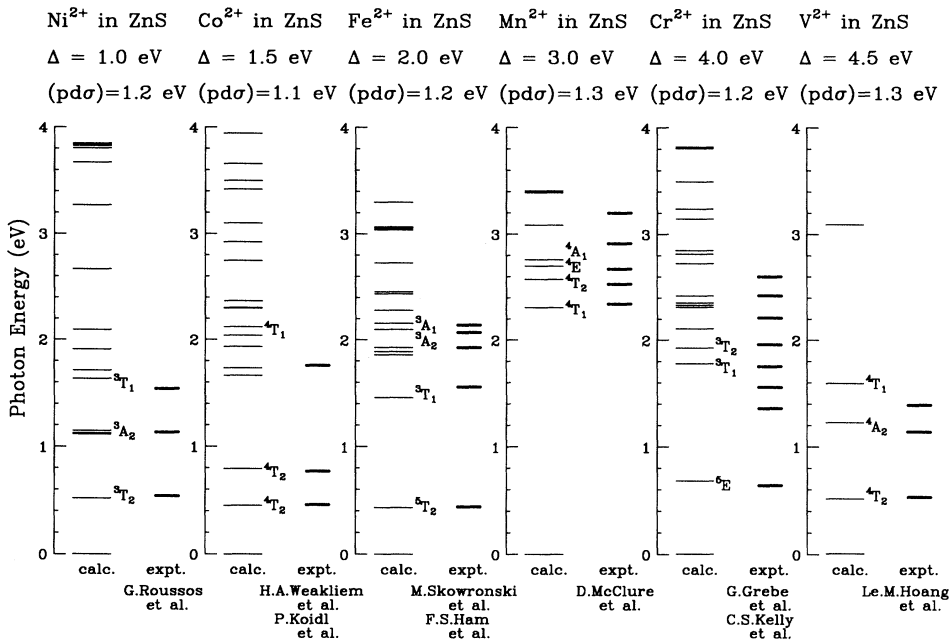


FIG. 3. Energy levels for various transition-metal impurities (from  $\text{V}^{2+}$  to  $\text{Ni}^{2+}$ ) in ZnS calculated using the CI cluster model compared with experimental  $d$ - $d$  optical-absorption spectra (Refs. 3 and 6–10).

photoemission spectra. The  $\varepsilon_v - \varepsilon_d$  values are thus nearly constant for different  $Y$ 's, whereas the  $\Delta_{\text{eff}}$  values obtained from photoemission spectra decrease in going from S to Se to Te.

#### D. Donor and acceptor ionization energies

When  $\Delta_{\text{eff}} < U_{\text{eff}}$ , the donor level has mainly  $d^n \underline{L}$  character and the acceptor level has mainly  $d^{n+1}$  character.

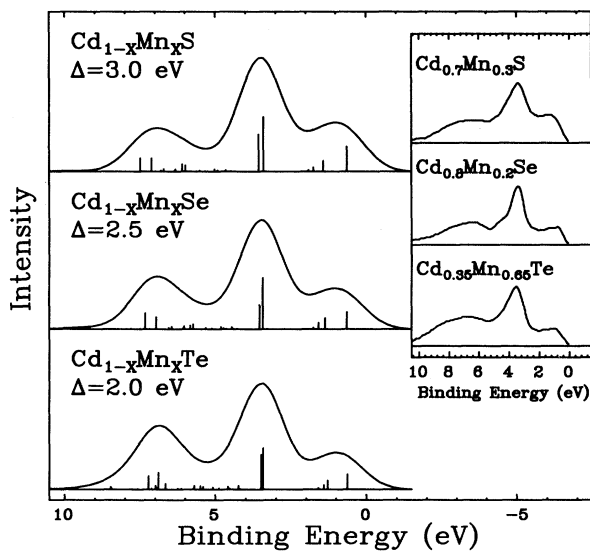


FIG. 4. Mn  $3d$ -derived photoemission spectra for  $\text{Cd}_{1-x}\text{Mn}_xY$  ( $Y=\text{S}, \text{Se}, \text{Te}$ ) calculated using the CI cluster model. Experimental results (Ref. 19) are shown in the inset. The calculated spectra are broadened with a Gaussian of 1.67 eV full width at half maximum. Binding energies are referenced to the valence-band maximum.

As can be seen from Table II, many transition-metal impurities in II-VI semiconductors satisfy this condition. Then the “effective Mott-Hubbard energy”  $U_{DA}$  (Fig. 1), defined as the difference between the donor and acceptor levels, is determined by  $\Delta_{\text{eff}}$  rather than  $U_{\text{eff}}$  (Ref. 27) and therefore  $d^n \underline{L}$ -like donor and  $d^{n+1}$ -like acceptor levels can be formed within the band gap in spite of the large  $U$ .<sup>15</sup> In order to study the  $d^n \underline{L}$ -like discrete states split off from the valence-band continuum, we have used an Anderson impurity model instead of the cluster model for an  $M^{2+}$  ion embedded in the filled host valence band.<sup>20,31</sup> In order to solve the problem numerically, the intra-atomic multiplet coupling is approximated by retaining

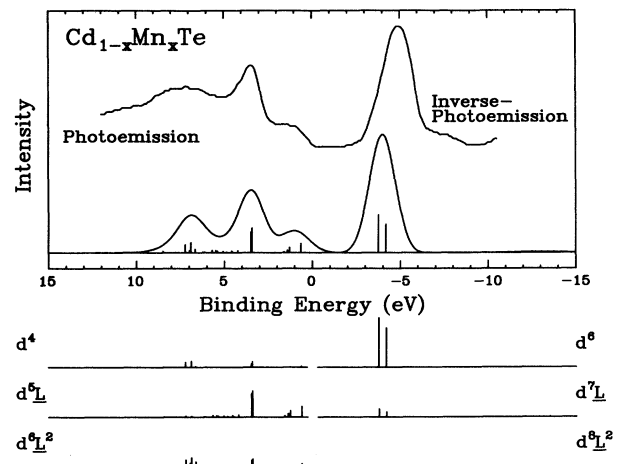


FIG. 5. Mn  $3d$ -derived photoemission (Ref. 19) and inverse-photoemission spectra (Ref. 28) for  $\text{Cd}_{1-x}\text{Mn}_x\text{Te}$  compared with those calculated using the CI cluster model. Energies are referenced to the valence-band maximum.

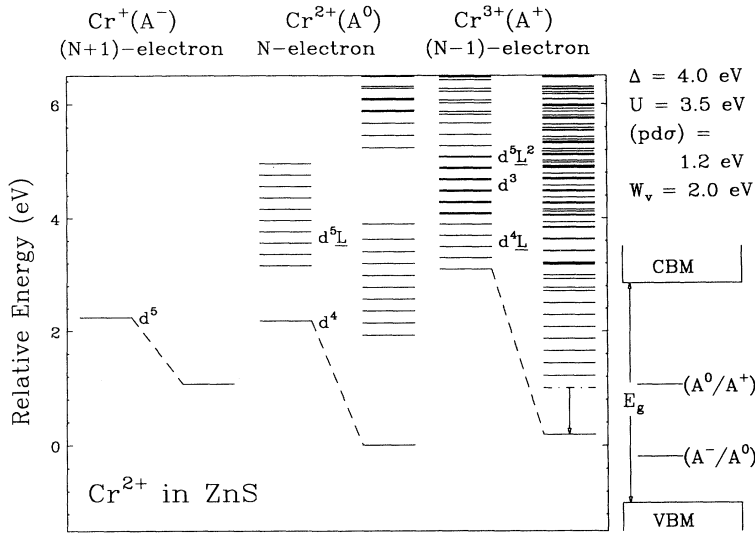


FIG. 6.  $(N-1)$ -electron ( $A^+$ ),  $N$ -electron ( $A^0$ ), and  $(N+1)$ -electron ( $A^-$ ) energy levels of a Cr impurity in ZnS calculated using the Anderson impurity model. The inset shows their mapping onto the one-electron energy-level scheme.

only the diagonal matrix elements in Kanamori's parametrization scheme.<sup>21</sup> As for the transfer integrals, we introduce  $V_{t2}(\epsilon) \equiv \langle t_2 | h | \underline{L}_{t2}(\epsilon) \rangle$  and  $V_e(\epsilon) \equiv \langle e | h | \underline{L}_e(\epsilon) \rangle$ , where  $\epsilon$  is the energy of the valence electron. The energy dependence of  $|V_{t2}(\epsilon)|^2$  and  $|V_e(\epsilon)|^2$  is assumed to be a semiellipsoid with an appropriate width  $W_v$ , which is taken to be  $\sim 2$  eV for the sulfides and selenides. Although the width of the valence band is 4–5 eV for ZnS or ZnSe studied here, host valence-band states within 2–3 eV of the valence-band maximum are found to predominantly contribute to the  $|V_{t2}(\epsilon)|^2$  and  $|V_e(\epsilon)|^2$ .<sup>32</sup> In actual calculations, the valence-band continuum is replaced by 10–20 discrete states, and  $\int |V_{t2}(\epsilon)|^2 d\epsilon$  and  $\int |V_e(\epsilon)|^2 d\epsilon$  are assumed to be equal to  $T_{t2}^2$  and  $T_e^2$ , respectively. Under this condition, the  $W_v \rightarrow 0$  limit corresponds to the cluster model.

As shown in Fig. 6, the  $\text{Cr}^{2+}$ , a  $d^4\bar{L}$ -like split-off state is formed well below the  $d^4\bar{L}$  continuum in the  $(N-1)$ -

electron state through the strong hybridization with the  $d^3$  state, which originally lies only  $U_{\text{eff}} - \Delta_{\text{eff}} \sim 1.1$  eV above the center of the  $d^4\bar{L}$  continuum. The split-off state corresponds to the donor level formed within the band gap. Since  $U_{DA} \sim \Delta_{\text{eff}}$  and the  $\Delta_{\text{eff}}$  is smaller than the band gap of ZnS, the lowest-energy level of the  $(N+1)$ -electron state or the acceptor level is located below the conduction-band minimum. We can map the donor and acceptor levels onto the one-electron energy-level scheme following the procedure described in Sec. II (see Fig. 1). On the other hand, in the  $(N-1)$ -electron state of  $\text{Mn}^{2+}$  in ZnS, a discrete state hardly splits off from the  $d^5\bar{L}$  continuum as shown in Fig. 7 because the  $d^4$  state is too far ( $U_{\text{eff}} - \Delta_{\text{eff}} \sim 3.2$  eV) above the lowest multiplet component of the  $d^5\bar{L}$  continua to induce a split-off state since the latter  $d^5\bar{L}$  component is stabilized by the exchange energy of the half-filled  $d^5$  shell. An acceptor level is not formed also within the band gap since

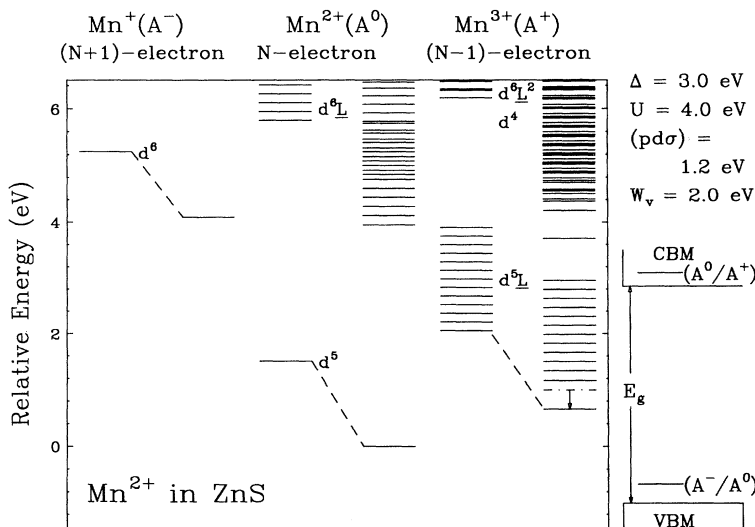


FIG. 7.  $(N-1)$ -electron ( $A^+$ ),  $N$ -electron ( $A^0$ ), and  $(N+1)$ -electron ( $A^-$ ) energy levels of a Mn impurity in ZnS calculated using the Anderson impurity model. The inset shows their mapping onto the one-electron energy-level scheme.

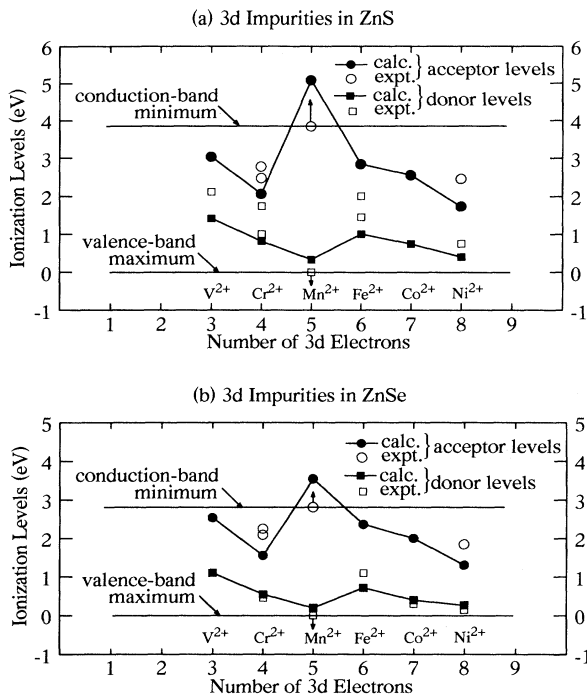


FIG. 8. Donor and acceptor ionization levels for various 3d transition-metal impurities in ZnS (a) and ZnSe (b) calculated using the Anderson impurity model. The calculations are compared with experimental values (Refs. 1 and 2).

the  $\Delta_{\text{eff}}$  is much larger than the band gap of ZnS.

In Fig. 8, the donor and acceptor ionization levels,  $\epsilon_c - E_D$  and  $\epsilon_v + E_A$ , calculated using the parameter sets in Table II are compared with experimental results.<sup>1,2</sup> The calculated values are generally in good agreement with the experimental results. For most of the transition-metal impurities, since the  $\Delta_{\text{eff}}$ 's are smaller than the band gaps of ZnS and ZnSe, the acceptor levels are located below the conduction-band minimum. The

calculated results explain the general lowering of the donor and acceptor levels with increasing atomic number of the transition-metal impurities as due to the monotonic decrease of  $\Delta$ . As mentioned above, on the other hand, the local maxima and minima at Cr, Mn, or Fe are attributed to the multiplet effects, which are reflected upon the nonmonotonic behavior of  $\Delta_{\text{eff}}$ .

#### IV. CONCLUSION

We have shown that the various experimental results on the 3d transition-metal impurities in II-VI semiconductors can be consistently explained in the CI picture: the  $d-d$  optical absorption, photoemission, and inverse-photoemission spectra and donor and acceptor ionization energies can be reproduced with a single set of parameters,  $\Delta$ ,  $U$ , and  $(pd\sigma)$ . The variation of the  $p-d$  exchange constant  $N\beta$  of  $\text{Cd}_{1-x}\text{Mn}_x\text{Y}$  ( $Y = \text{S, Se, Te}$ ) on the anion  $Y$  is also explained. It is shown that the physical properties are controlled both by the smooth variation of  $\Delta$  as a function of impurity atomic number and by the apparently irregular variation of  $\Delta_{\text{eff}}$  due to the multiplet effects. Application of the present method to a wider range of impurity systems, e.g., impurities in more covalent hosts such as III-V semiconductors, as well as to the calculation of other physical properties such as the  $g$  values and the hyperfine-coupling constants remain to be made in future.

#### ACKNOWLEDGMENTS

The authors would like to thank Professor M. Taniguchi and Professor K. Sato for many useful discussions. All the calculations in this work were performed on a VAX computer in Meson Science Laboratory, Faculty of Science, University of Tokyo. One of us (T.M.) is supported by the Japan Society for the Promotion of Science for Japanese Junior Scientists. The present work is supported by the Grants-in-Aid for Scientific Research from the Ministry of Education, Science and Culture and Toray Science Foundation.

<sup>1</sup>For review and references, see A. Zunger, in *Solid State Physics*, edited by H. Ehrenreich and D. Turnbull (Academic, New York, 1986), Vol. 39, p. 275.

<sup>2</sup>A. Fazzio, M. J. Caldas, and A. Zunger, *Phys. Rev. B* **30**, 3430 (1984).

<sup>3</sup>D. S. McClure, *J. Chem. Phys.* **39**, 2850 (1963).

<sup>4</sup>D. W. Langer and H. J. Richer, *Phys. Rev.* **146**, 554 (1966).

<sup>5</sup>Y. R. Lee and A. K. Ramdas, *Solid State Commun.* **51**, 861 (1984).

<sup>6</sup>G. Roussos and H. R. Schulz, *Phys. Status Solidi B* **100**, 577 (1980).

<sup>7</sup>H. A. Weakliem, *J. Chem. Phys.* **36**, 2117 (1962); P. Koidl, O. F. Schirmer, and U. Kaufmann, *Phys. Rev. B* **8**, 4926 (1973).

<sup>8</sup>M. Skowronski and Z. Liro, *J. Phys. C* **15**, 137 (1982); F. S. Ham and G. A. Slack, *Phys. Rev. B* **4**, 777 (1971).

<sup>9</sup>C. S. Kelly and F. Williams, *Phys. Rev. B* **2**, 3 (1970); G. Grebe and H. J. Schulz, *Phys. Status Solidi B* **54**, K69 (1972); G.

Grebe, G. Roussos, and H. J. Schulz, *J. Phys. C* **9**, 4511 (1976).

<sup>10</sup>Le. M. Hoang and J. M. Baranowski, *Phys. Status Solidi B* **84**, 361 (1977).

<sup>11</sup>S. Sugano, Y. Tanabe, and H. Kamimura, *Multiplets of Transition Metal Ions in Crystals* (Academic, New York, 1970); J. S. Griffith, *The Theory of Transition Metal Ions* (Cambridge, London, 1971).

<sup>12</sup>S. Watabnabe and H. Kamimura, *J. Phys. Soc. Jpn.* **56**, 1078 (1987).

<sup>13</sup>H. Katayama-Yoshida and A. Zunger, *Phys. Rev. B* **33**, 2961 (1986).

<sup>14</sup>A. Oshiyama, N. Hamada, and H. Katayama-Yoshida, *Phys. Rev. B* **37**, 1395 (1988).

<sup>15</sup>F. D. M. Haldane and P. W. Anderson, *Phys. Rev. B* **13**, 2553 (1976).

<sup>16</sup>G. Picoli and A. Chomette, *Phys. Rev. B* **30**, 7138 (1984).

- <sup>17</sup>For review and references of diluted magnetic semiconductor, see J. K. Furdyna, *J. Appl. Phys.* **64**, R29 (1988).
- <sup>18</sup>M. Taniguchi, L. Ley, R. J. Johnson, J. Ghijsen, and M. Cardona, *Phys. Rev. B* **33**, 1206 (1986).
- <sup>19</sup>L. Ley, M. Taniguchi, J. Ghijsen, R. L. Johnson, and A. Fujimori, *Phys. Rev. B* **35**, 2839 (1987); M. Taniguchi, A. Fujimori, M. Fujisawa, T. Mori, I. Souma, and Y. Oka, *Solid State Commun.* **62**, 431 (1987).
- <sup>20</sup>O. Gunnarsson, O. K. Anderson, O. Jepsen, and J. Zaanen, *Phys. Rev. B* **39**, 1708 (1989).
- <sup>21</sup>A. E. Bocquet, T. Mizokawa, T. Saitoh, H. Namatame, and A. Fujimori, *Phys. Rev. B* **46**, 3771 (1992); A. E. Bocquet, T. Saitoh, T. Mizokawa, and A. Fujimori, *Solid State Commun.* **83**, 11 (1992).
- <sup>22</sup>A. Fujimori and F. Minami, *Phys. Rev. B* **30**, 957 (1984).
- <sup>23</sup>A. Bouhelal and J. P. Albert, *Solid State Commun.* **69**, 713 (1989).
- <sup>24</sup>W. A. Harrison, *Electronic Structure and the Properties of Solids* (Dover, New York, 1989).
- <sup>25</sup>O. Gunnarsson and O. Jepsen, *Phys. Rev. B* **38**, 3568 (1988).
- <sup>26</sup>S. Mochizuki, B. Piriou, and J. Dexpert-Ghys, *J. Phys. Condens. Matter* **2**, 5225 (1990).
- <sup>27</sup>J. Zaanen, G. A. Sawatzky, and J. W. Allen, *Phys. Rev. Lett.* **55**, 418 (1985); S. Hüfner, *Z. Phys. B* **61**, 135 (1985).
- <sup>28</sup>A. Franciosi, A. Wall, Y. Gao, J. H. Weaver, M. H. Tai, J. D. Dow, R. U. Kasowski, R. Reifenberger, and F. Pool, *Phys. Rev. B* **40**, 12009 (1989).
- <sup>29</sup>S.-H. Wei and A. Zunger, *Phys. Rev. Lett.* **56**, 2391 (1986); *Phys. Rev. B* **35**, 2340 (1987).
- <sup>30</sup>B. E. Larson, K. C. Hass, H. Ehrenreich, and A. E. Carlsson, *Phys. Rev. B* **37**, 4137 (1988); K. C. Hass, in *Semimagnetic Semiconductors and Diluted Magnetic Semiconductors*, edited by M. Averous and M. Balkanski (Plenum, New York, 1991), p. 59.
- <sup>31</sup>J. Zaanen, thesis, University of Groningen, 1986.
- <sup>32</sup>We have confirmed using a tight-binding model that a band with relatively small dispersion  $\sim 2-3$  eV, which is mainly constructed from anion  $p$  and cation  $s$  orbitals, strongly hybridizes with the impurity  $3d$  orbitals.

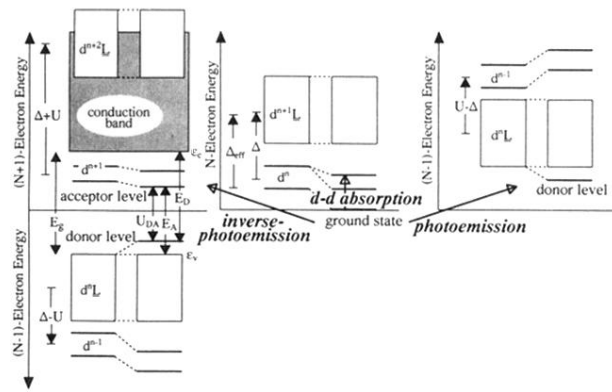


FIG. 1. Schematic energy-level diagrams from a  $d^n$  transition-metal impurity in a II-VI semiconductor, including hybridization between the 3d and host valence band. For clarity, higher-order charge-transfer states (e.g.,  $d^{n+2}\underline{L}^2$  in the  $N$ -electron states) are not shown.